Available online at http://scik.org
Commun. Math. Biol. Neurosci. 2023, 2023:97
https://doi.org/10.28919/cmbn/8154
ISSN: 2052-2541

MODELING AND STABILITY ANALYSIS OF CRYPTOSPORIDIOSIS TRANSMISSION DYNAMICS WITH BEDDINGTON-DEANGELIS INCIDENCE

AUBIN NANA MBAJOUN[1,*], RAOUL DOMINGO AYISSI[2], SAMUEL MUTUA[3]

[1]Department of Mathematics, Pan African University Institute for Basic Sciences Technology and Innovation (PAUSTI), Nairobi, Kenya

[2]Department of Mathematics and Physics, National Advanced School of Engineering University of Yaounde I, P.O. Box : 812 Yaounde, Cameroon

[3]Department of Mathematics, Statistics and Physical Sciences, Taita Taveta University, P.O.Box 635-80300, Kenya

Abstract. In this paper, a model describing the dynamics of Cryptosporidiosis is developed and analysed using ordinary differential equations with a non linear incidence called Beddington-DeAngelis function. We computed the basic reproduction number ($\mathscr{R}_{ha}$) using the next generation matrix method and carry out the stability analysis of the model equilibria. We applied the center manifold theory to investigate the local stability of the endemic equilibrium and found that the model exhibits a forward bifurcation at $\mathscr{R}_{ha} = 1$. Further, the global stability of the endemic equilibrium is obtained under a certain condition using Lyapunov's method and LaSalle'S invariance principle. The most sensitive parameters on the model outcome are also identified using the normalized forward sensitivity index. Finally, we performed numerical simulations and displayed then graphically to validate our analytical results, and the epidemiological implications of the key out comes were briefly discussed.

Keywords: cryptosporidiosis model; basic reproduction number; Beddington-DeAngelis incidence; stability analysis; forward bifurcation.

2020 AMS Subject Classification: 92C60.

*Corresponding author
E-mail address: naubin463@yahoo.com
Received July 27, 2023

1. INTRODUCTION

Cryptosporidiosis is an infection caused by an apicomplexan protozoan known as Cryptosporidium. Cryptosporidium common parasites of vertebrates have recently attracted increasing interest due to several serious waterborne outbreaks, and the life-threatening nature of infection in immunocompromised patients, children, the elderly, and patients on chemotherapy, pregnant women; and also the realization of economic losses caused by these pathogens in livestock. It is a common enteric pathogen in humans and domestic animals worldwide with a very low infective dose of one to ten ooysts (Pereira [1]). The sporulated ooysts are immediately infectious when excreted in faeces as there is no intermediate host. Cattle are reared throughout Cameroon but the major production areas are in the West and North West Regions and from the Adamawa Province [2]. The cattle are transported on foot to the cattle market and the dung they pass along the road is likely to contaminate the environment and the oocysts possibly end up in streams after torrential rains. In time past, following the description of Cryptosporidium in mice by Ernest Edward Tyzzer [3], the genus Cryptosporidium has been studied, and now discovered to contain numerous species and genotypes adapted to parasitic life in almost all classes of vertebrates. Over the years, our knowledge has expanded from microscopic observations of infection and environmental contamination to the knowledge obtained from large application spread of molecular techniques to taxonomy and epidemiology. Although, the medical and veterinary significance of this protozoan was not fully appreciated for an- other 70 years. The interest in Cryptosporidium escalated tremendously over the last two and half decades [4, 5]. It was later recognized as a cause of disease in 1976. As several methods were developed to analyze stool samples, the protozoa was increasingly reported as the cause of human disease [6]. At first, Crypto was categorized as a veterinary problem because, majority of the early cases were diagnosed due to individuals rearing farm animals such as cows. Furthermore, 155 species of animals specifically mammals have been reported to be infected with Cryptosporidium parvum which is also known as C. parvum [7]. Among the 15 named species of Cryptosporidium infectious to non-human vertebrate hosts C. Baileyi, C. canis, C. felis, C. hominis, C meleagridis, C. muris, and C. parvum have been reported to also infect humans. The primary hosts for C. hominis are Humans, except for C. parvum, which is widespread in non-human hosts and is the most frequently reported zoonotic species, the remaining species left have been reported primarily in immunocompromised or immunosuppressed humans [7]. The first Cryptosporidiosis outbreak that was widely known occurred in 1987 [8] in Carrollton, Georgia. About 13,000 persons became sick as a result of the outbreak the disease. The main cause was traced to a large contaminated water system. In 1993, in Milwaukee area, Wisconsin, a massive outbreak of the disease occurred, causing approximately 400,000 people to fell sick as a result of contaminated drinking water in one of the two treatment plants serving the Milwaukee area [6]. Therefore, motivated by the above discussion into account, in this paper, we propose and analyze a mathematical model of Cryptosporidiosis disease dynamics in humans and animals population with the Beddington-DeAngelis incidence . We construct the compartmental model by considering three different classes of individuals in the humans population and three different classes of individuals in the animals population. We believe that the findings of our work will be helpful in indicating appropriate measures to control the spread of the disease. The rest of the paper is organized as follows: The model description and formulation are discussed in Section 2. The basic properties of the model including non-negativity and boundedness of solutions, the mathematical analysis of the model including the introduction of the threshold parameter $\mathscr{R}_{ha}$ obtained using the Next-Generation method, the stability of the disease-free and endemic- equilibrium points as well as the bifurcation and sensitivity analysis are investigated in Section 3. In Section 4, we perform numerical simulations to support some of the analytical results. A brief discussion and conclusions are presented in the last section.

2. Description and Formulation of the Model

2.1. Assumptions.

The following assumptions will be used to simplify the model :

- In the presence of the disease we divide the model into two parts, the total human and total animal (vector). These populations at any time, are also divided into six sub populations (compartments). The total human population also represented by H divided into sub-populations of susceptible humans H_S, infected humans H_I and recovered humans H_R. The total human population is given by : $H(t) = H_S(t) + H_I(t) + H_R(t)$. The total animal population, represented by A, is divided into sub-populations of susceptible animals A_S, infected animals A_I and recovered animals A_R. The total animal population becomes $A(t) = A_S(t) + A_I(t) + A_R(t)$.

- A susceptible human can be infected only by an infected animal.
- A susceptible animal can be infected only by an infected animal.
- The force of infection from infected animals to susceptible humans is modeling using Beddington-DeAngelis incidence form as $\frac{\delta_1 H_S(t)A_I(t)}{1+m_1H_S(t)+m_2A_I(t)}$ and $\frac{\delta_2 A_S(t)A_I(t)}{1+m_3A_S(t)+m_4A_I(t)}$ from infected animal to susceptible animal where δ_1 and δ_2 are infection rate, m_1, m_2, m_3 and m_4 are parameters that measure the inhibitory effect.

2.2. The model derivation. Our proposed model divides the total human population $H(t)$ into three subclasses of susceptible $H_S(t)$, infected $H_I(t)$ and recovered $H_R(t)$.The total animal population $A(t)$ is divided into three subclasses of susceptible $A_S(t)$, infected $A_I(t)$ and recovered $A_R(t)$. For the model susceptible humans $H_S(t)$ are recruited at a rate Λ_H, infected at a rate $\frac{\delta_1 H_S(t)A_I(t)}{1+m_1H_S(t)+m_2A_I(t)}$ and die naturally at a rate μ_H. Infected humans $H_I(t)$ are recruited at a rate $\frac{\delta_1 H_S(t)A_I(t)}{1+m_1H_S(t)+m_2A_I(t)}$, die naturally at a rate μ_H, die from infection at a rate α_H, recover and has permanent immunity at a rate β_H. Recovered humans are recruited at a rate β_H and die naturally at a rate μ_H. Susceptible animals $A_S(t)$ are recruited at a rate Λ_A, infected at a rate $\frac{\delta_2 A_S(t)A_I(t)}{1+m_3A_S(t)+m_4A_I(t)}$ and die naturally at a rate μ_A. Infected animals $A_I(t)$ are recruited at a rate $\frac{\delta_2 A_S(t)A_I(t)}{1+m_3H_S(t)+m_4A_I(t)}$, die naturally at a rate μ_A, die from infection at a rate α_A, recover and has permanent immunity at a rate β_A. Recovered animals are recruited at a rate β_A and die naturally at a rate μ_A. The parameters of the model is summarized in Table 1 and the flow diagram of the model is shown in Figure 1.

Table 1. Notations and Description of model (1) parameters

Parameter	Description
δ_1	Infection or predation rate of infected animals on susceptible humans
δ_2	Infection or predation rate of infected animals on susceptible animals
$m_i (i = 1,2,3,4)$	are parameters that measure the inhibitory effect
Λ_H	Human recruitment rate
μ_H	Human natural death rate
α_H	Human cryptosporidiosis induced death rate
β_H	Human recovery rate
Λ_A	Animal recruitment rate
μ_A	Animal natural death rate
α_A	Animal cryptosporidiosis induced death rate
β_A	Animal recovery rate

Based on the above description, we have the following compartmental diagram for the transmission dynamics of Cryptosporidiosis

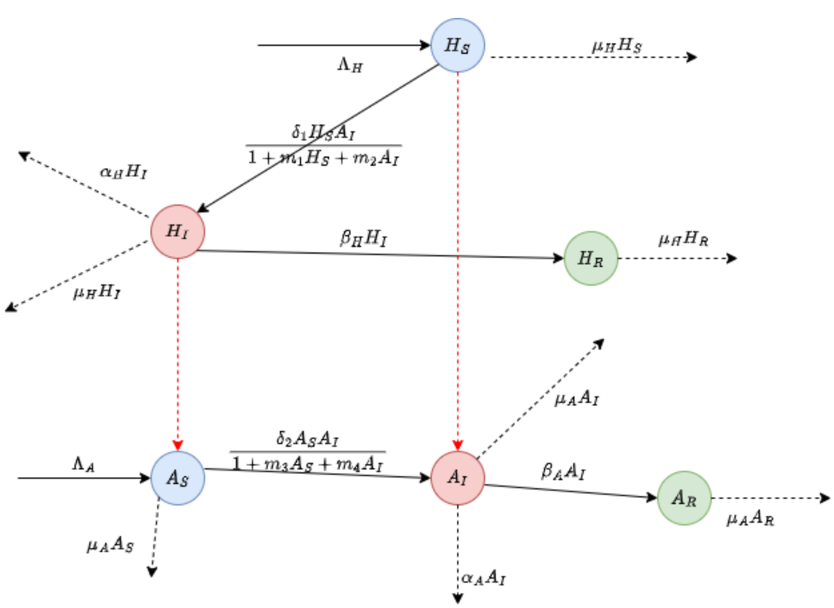

FIGURE 1. Flow diagram for the Cryptosporidiosis disease transmission dynamics

Thus, from the above discussions, the model describing the transmission dynamics of Cryptosporidiosis disease can be formulated mathematically by the following deterministic system of nonlinear differential equations:

$$\begin{cases} \frac{dH_S(t)}{dt} = \Lambda_H - \mu_H H_S(t) - \frac{\delta_1 H_S(t)A_I(t)}{1+m_1H_S(t)+m_2A_I(t)} \\ \frac{dH_I(t)}{dt} = \frac{\delta_1 H_S(t)A_I(t)}{1+m_1H_S(t)+m_2A_I(t)} - (\alpha_H+\mu_H+\beta_H)H_I(t) \\ \frac{dH_R(t)}{dt} = \beta_H H_I(t) - \mu_H H_R(t) \\ \frac{dA_S(t)}{dt} = \Lambda_A - \mu_A A_S(t) - \frac{\delta_2 A_S(t)A_I(t)}{1+m_3A_S(t)+m_4A_I(t)} \\ \frac{dA_I(t)}{dt} = \frac{\delta_2 A_S(t)A_I(t)}{1+m_3A_S(t)+m_4A_I(t)} - (\alpha_A+\mu_A+\beta_A)A_I(t) \\ \frac{dA_R(t)}{dt} = \beta_A A_I(t) - \mu_A A_R(t) \end{cases} \tag{1}$$

with initial condition $H_S(0) \geq 0,\ H_I(0) \geq 0,\ H_R(0) \geq 0,\ A_S(0) \geq 0,\ A_I(0) \geq 0,\ A_R(0) \geq 0.$

3. Cryptosporidiosis Model Analysis

3.1. Positivity and boundedness of solutions.

In this subsection, we must prove that at $t \geq 0$ all solutions of the model system (1) are positive and bounded for the Cryptosporidiosis model to be meaningful and well posed.

Theorem 3.1 A non-negative solution $(H_S(t),H_I(t),H_R(t),A_S(t),A_I(t),A_R(t))$ for model (1) exists for all states with positive initial conditions ($H_S(0) \geq 0,\ H_I(0) \geq 0,\ H_R(0) \geq 0, A_S(0) \geq 0,\ A_I(0) \geq 0,\ A_R(0) \geq 0$) for all $t \geq 0$.

Proof. According to the first equation of the system of differential equation (1) we have:

$\frac{dH_S(t)}{dt} \geq -H_S(t)\left(\mu_H + \frac{\delta_1 H_S(t)A_I(t)}{1+m_1H_S(t)+m_2A_I(t)}\right)$

that is:

$\frac{dH_S(t)}{H_S(t)} \geq -\left(\mu_H + \frac{\delta_1 H_S(t)A_I(t)}{1+m_1H_S(t)+m_2A_I(t)}\right)dt$

that is:

$\frac{dH_S(t)}{H_S(t)} \geq -(\mu_H + f(H_S,A_I)\,dt$ where $f(H_S,A_I) = \frac{\delta_1 A_I(t)}{1+m_1H_S(t)+m_2A_I(t)}$

The integration of the inequality gives

$H_S(t) \geq H_S(0)e^{-\int_0^t(\mu_H+f(H_S(\varepsilon),A_I(\varepsilon)))d\varepsilon} > 0$ since $H_S(0) > 0$.

According to the second equation of the system of differential equation (1) we have:

$\frac{dH_I(t)}{dt} \geq -(\alpha_H + \mu_H + \beta_H)dt$ and integration of inequality gives
$H_I(t) \geq H_I(0)e^{-(\alpha_H+\mu_H+\beta_H)t} > 0$ since $H_I(0) > 0$.

Let us take the third equation we have:
$\frac{dH_R(t)}{H_R(t)} \geq -\mu_H dt$ that is $H_R(t) \geq H_R(0)e^{-(\mu_H)t} > 0$ since $H_R(0) > 0$.
Similarly, using the same argument, it can be shown that
$A_S(t) \geq A_S(0)e^{-\int_0^t(\mu_A+g(A_S(\varepsilon),A_I(\varepsilon)))d\varepsilon} > 0$ since $A_S(0) > 0$ with $g(A_S,A_I) = \frac{\delta_2 A_I(t)}{1+m_3A_S(t)+m_4A_I(t)}$, $A_I(t) \geq A_I(0)e^{-(\alpha_A+\mu_A+\beta_A)t} > 0$ since $A_I(0) > 0$, $A_R(t) \geq A_R(0)e^{-(\mu_A)t} > 0$ since $A_R(0) > 0$ and this completes the proof of the Theorem 3.1.

Theorem 3.2 The solution of the model system (1) with positive initial conditions are ultimately bounded in $\Omega \subset \mathbb{R}^3 \times \mathbb{R}^3$.

Proof. Human population at any time, t is given by: $H(t) = H_S(t) + H_I(t) + H_R(t)$

so

$$\begin{aligned}\frac{dH(t)}{dt} &= \frac{dH_S(t)}{dt} + \frac{dH_I(t)}{dt} + \frac{dH_R(t)}{dt}\\ &= \Lambda_H - \alpha_H H_I(t) - \mu_H\left(H_S(t)+H_I(t)+H_R(t)\right)\\ &= \Lambda_H - \alpha_H H_I(t) - \mu_H H(t)\end{aligned}$$

In the absence of mortality due to Cryptosporidiosis infection we obtain $\frac{dH(t)}{dt} \leq \Lambda_H - \mu_H H(t)$, that is $\frac{dH(t)}{\Lambda_H - \mu_H H(t)} \leq dt$, so we obtain $\Lambda_H - \mu_H H(t) \geq C_1 e^{-\mu_H t}$ where C_1 is a constant. At $t = 0$, we have $C_1 = \Lambda_H - \mu_H H(0)$, so $\Lambda_H - \mu_H H(t) \geq (\Lambda_H - \mu_H H(0))\, e^{-\mu_H t}$, that is $H(t) \leq \frac{\Lambda_H}{\mu_H} - \left(\frac{\Lambda_H}{\mu_H} - H(0)\right) e^{-\mu_H t}$. As $t \to \infty$, we obtain $H(t) \to \frac{\Lambda_H}{\mu_H}$, therefore $0 \leq H(t) \leq \frac{\Lambda_H}{\mu_H}$. We define

$$\Omega_1 = \left\{(H_S(t),H_I(t),H_R(t)) \in \mathbb{R}^3_+ : 0 \leq H_S(t)+H_I(t)+H_R(t) \leq \frac{\Lambda_H}{\mu_H}\right\}$$

Animal population at any time t is given by: $A(t) = A_S(t) + A_I(t) + A_R(t)$. Similarly we get $0 \leq A(t) \leq \frac{\Lambda_A}{\mu_A}$ and we define

$$\Omega_2 = \left\{(A_S(t),A_I(t),A_R(t)) \in \mathbb{R}^3_+ : 0 \leq A_S(t)+A_I(t)+A_R(t) \leq \frac{\Lambda_A}{\mu_A}\right\}$$

Therefore the feasible solution set of Cryptosporidiosis model (1) remain in the following region $\Omega = \Omega_1 \times \Omega_2$. Thus, the Cryptosporidiosis model (1) is well posed epidemiologically and mathematically. Hence, it is sufficient to study the dynamics of the Cryptosporidiosis model in Ω.

3.2. Disease-Free Equilibrium point. The disease-free equilibrium point (DFE) is the point at which no disease is present in the population of human and animal. However, DFE is obtain by setting $H_I(t) = H_R(t) = 0$ and $A_I(t) = A_R(t) = 0$. The DFE of the Cryptosporidiosis model (1) is given by:

$$E_0 = \left\{ \frac{\Lambda_H}{\mu_H}, 0, 0, \frac{\Lambda_A}{\mu_A}, 0, 0 \right\} \tag{2}$$

3.3. Basic reproduction number ($\mathscr{R}_{ha}$). Using the "Next Generation Matrix" approach, we determine $\mathscr{R}_{ha}$ and its linear stability. Basic reproduction number refers to the number of secondary cases produced on average by one infected animal or person in completely susceptible population. This combines the biology of infections with the social and behavioural factors influencing contact rate [9, 10, 11]. It is the threshold parameter that determines or governs the spread of disease. Considering only the infection classes in the system (1)

$$\frac{dH_I(t)}{dt} = \frac{\delta_1 H_S(t) A_I(t)}{1 + m_1 H_S(t) + m_2 A_I(t)} - (\alpha_H + \mu_H + \beta_H) H_I(t) \tag{3}$$

$$\frac{dA_I(t)}{dt} = \frac{\delta_2 A_S(t) A_I(t)}{1 + m_3 A_S(t) + m_4 A_I(t)} - (\alpha_A + \mu_A + \beta_A) A_I(t) \tag{4}$$

Let F be the number of new infection coming into the system and V be the number of infections that are leaving the system either by death or birth, then

$$F = \begin{bmatrix} \frac{\delta_1 H_S(t) A_I(t)}{1+m_1 H_S(t)+m_2 A_I(t)} \\ \frac{\delta_2 A_S(t) A_I(t)}{1+m_3 A_S(t)+m_4 A_I(t)} \end{bmatrix} \tag{5}$$

and

$$V = \begin{bmatrix} (\alpha_H + \mu_H + \beta_H) H_I(t) \\ (\alpha_A + \mu_A + \beta_A) A_I(t) \end{bmatrix} \tag{6}$$

The jacobian matrix of F and V at disease-free equilibrium is obtained by f and v as follows:

$$f = \begin{bmatrix} 0 & \frac{\delta_1 \Lambda_H}{\mu_H + m_1 \Lambda_H} \\ 0 & \frac{\delta_2 \Lambda_A}{\mu_A + m_3 \Lambda_A} \end{bmatrix} \tag{7}$$

and

$$v = \begin{bmatrix} \alpha_H + \mu_H + \beta_H & 0 \\ 0 & \alpha_A + \mu_A + \beta_A \end{bmatrix} \tag{8}$$

The inverse of v is found to be

$$v^{-1} = \begin{bmatrix} \frac{1}{\alpha_H+\mu_H+\beta_H} & 0 \\ 0 & \frac{1}{\alpha_A+\mu_A+\beta_A} \end{bmatrix} \tag{9}$$

The next generation matrix fv^{-1} is given by :

$$fv^{-1} = \begin{bmatrix} 0 & \frac{\delta_1\Lambda_H}{(\mu_H+m_1\Lambda_H)(\alpha_H+\mu_H+\beta_H)} \\ 0 & \frac{\delta_2\Lambda_A}{(\mu_A+m_3\Lambda_A)(\alpha_A+\mu_A+\beta_A)} \end{bmatrix} \tag{10}$$

By finding the eigenvalues of matrix fv^{-1} we get

$$\lambda_1 = 0,\ \lambda_2 = \frac{\delta_2\Lambda_A}{(\mu_A + m_3\Lambda_A)(\alpha_A + \mu_A + \beta_A)} \tag{11}$$

Then

$$\mathscr{R}_{ha} = max(\lambda_1, \lambda_2) = \frac{\delta_2\Lambda_A}{(\mu_A + m_3\Lambda_A)(\alpha_A + \mu_A + \beta_A)} \tag{12}$$

3.4. Local stability of the disease-free equilibrium. Local stability of the disease-free equilibrium is given by Theorem 3.3

Theorem 3.3 The disease-free equilibrium is locally asymptotically stable if $\mathscr{R}_{ha} < 1$ and unstable if $\mathscr{R}_{ha} > 1$.

Proof. The disease-free equilibrium point E_0 is locally asymptotically stable if the real parts of the eigenvalues of the jacobian matrix corresponding to the system (1) around the DFE are all negatives. The Jacobian matrix corresponding to the system (1) around E_0 is given by:

$$J(E_0) = \begin{pmatrix} -\mu_H & 0 & 0 & 0 & \frac{-\delta_1\Lambda_H}{\mu_H+m_1\Lambda_H} & 0 \\ 0 & -(\alpha_H + \mu_H + \beta_H) & 0 & 0 & \frac{\delta_1\Lambda_H}{\mu_H+m_1\Lambda_H} & 0 \\ 0 & \beta_H & -\mu_H & 0 & 0 & 0 \\ 0 & 0 & 0 & -\mu_A & \frac{-\delta_2\Lambda_A}{\mu_A+m_3\Lambda_A} & 0 \\ 0 & 0 & 0 & 0 & \frac{\delta_2\Lambda_A}{\mu_A+m_3\Lambda_A} - (\alpha_A + \mu_A + \beta_A) & 0 \\ 0 & 0 & 0 & 0 & \beta_A & -\mu_A \end{pmatrix} \tag{13}$$

The characteristic equation of the Jacobian matrix (13) is given by:

$$(a-\lambda)(b-\lambda)(c-\lambda)(d-\lambda)(e-\lambda)(h-\lambda)=0 \tag{14}$$

where $a=-\mu_H$, $b=-(\alpha_H+\mu_H+\beta_H)$, $c=-\mu_H$, $d=-\mu_A$, $e=\frac{\delta_2\Lambda_A}{\mu_A+m_3\Lambda_A}-(\alpha_A+\mu_A+\beta_A)$, $h=-\mu_A$.

Therefore the eigenvalues are a, b, c, d, e and h. Clearly, a, b, c, d and h are negative.

If $e<0$, that is $\frac{\delta_2\Lambda_A}{\mu_A+m_3\Lambda_A}-(\alpha_A+\mu_A+\beta_A)<0$, that is $\frac{\delta_2\Lambda_A}{\mu_A+m_3\Lambda_A}<\alpha_A+\mu_A+\beta_A$, that is $\mathscr{R}_{ha}<1$. If $e>0$ we have $\mathscr{R}_{ha}>1$. Therefore E_0 is locally asymptotically stable if $\frac{\delta_2\Lambda_A}{\mu_A+m_3\Lambda_A}<\alpha_A+\mu_A+\beta_A$ whenever $\mathscr{R}_{ha}<1$.

3.5. Global stability of the disease-free equilibrium point. In this section we investigate global asymptotic stability of the disease-free equilibrium point using the theorem by Castillo-Chavez and Song [12] as done in [13]. To do so, we write system equation (1) as:

$$\begin{cases} \frac{dX}{dt}=F(X,Y) \\ \frac{dY}{dt}=G(X,Y),\ G(X,0)=0 \end{cases} \tag{15}$$

Where $X=(H_S(t),H_R(t),A_S(t),A_R(t))\in\mathbb{R}^4$ denotes uninfected population and $Y=(H_I(t),A_I(t))\in\mathbb{R}^2$ represents the infected population. Let X^* be the disease-free equilibrium of the system

$$\frac{dX}{dt}=F(X,0) \tag{16}$$

Then $X^*=\left(\frac{\Lambda_H}{\mu_H},0,\frac{\Lambda_A}{\mu_A},0\right)$. The DFE of the model is $E_0=(X^*,0)=\left(\frac{\Lambda_H}{\mu_H},0,0,\frac{\Lambda_A}{\mu_A},0,0\right)$. Furthermore, we list two conditions and if met will guarantee the global asymptotic stability of E_0.

(i) For $\frac{dX}{dt}=F(X,0)$, X^* is globally asymptotically stable;

(ii) $\frac{dY}{dt}=D_YG(X^*,0)Y-\hat{G}(X,Y)$, $\hat{G}(X,Y)\geq 0$ for all $(X,Y)\in\Omega$, where $D_YG(X^*,0)$ is a Metzler and the Jacobian matrix of $G(X,Y)$ taken in (H_I,A_I) and evaluated at $E_0=(X^*,0)$.

Theorem 3.4 The disease-free equilibrium point $E_0=(X^*,0)$ is globally asymptotically stable for the model (1) provided that $\mathscr{R}_{ha}<1$ and that the conditions (i) and (ii) are satisfied.

Proof. We only need to show that the conditions (i) and (ii) hold when $\mathscr{R}_{ha} < 1$. From the model system (1) we obtain $F(X,Y)$ and $G(X,Y)$ as :

$$F(X,Y) = \begin{pmatrix} \Lambda_H - \mu_H H_S(t) - \frac{\delta_1 H_S(t) A_I(t)}{1+m_1 H_S(t)+m_2 A_I(t)} \\ \beta_H H_I(t) - \mu_H H_R(t) \\ \Lambda_A - \mu_A A_S(t) - \frac{\delta_2 A_S(t) A_I(t)}{1+m_3 A_S(t)+m_4 A_I(t)} \\ \beta_A A_I(t) - \mu_A A_R(t) \end{pmatrix} \tag{17}$$

$$G(X,Y) = \begin{pmatrix} \frac{\delta_1 H_S(t) A_I(t)}{1+m_1 H_S(t)+m_2 A_I(t)} - (\alpha_H + \mu_H + \beta_H) H_I(t) \\ \frac{\delta_2 A_S(t) A_I(t)}{1+m_3 A_S(t)+m_4 A_I(t)} - (\alpha_A + \mu_A + \beta_A) A_I(t) \end{pmatrix} \tag{18}$$

From condition (i), we consider the reduced system $\frac{dX}{dt} = F(X,0)$ and we get:

$$\begin{cases} \frac{dH_S(t)}{dt} = \Lambda_H - \mu_H H_S(t) \\ \frac{dH_R(t)}{dt} = -\mu_H H_R(t) \\ \frac{dA_S(t)}{dt} = \Lambda_A - \mu_A A_S(t) \\ \frac{dA_R(t)}{dt} = -\mu_A A_R(t) \end{cases} \tag{19}$$

$X^* = \left(\frac{\Lambda_H}{\mu_H}, 0, \frac{\Lambda_A}{\mu_A}, 0\right)$ is globally asymptotically stable equilibrium point for the reduced system $\frac{dX}{dt} = F(X,0)$. We proved this by finding the solution of the equations in the system (19).
From the second and fourth equations of (19), we have $H_R(t) = H_{R,0}\, e^{-\mu_H t}$, which approaches 0 as $t \to \infty$, $H_{R,0}$ is a constant and $A_R(t) = A_{R,0}\, e^{-\mu_A t}$, which approaches 0 as $t \to \infty$, $A_{R,0}$ is a constant. From the first and third equations of (19), we have $H_S(t) = \frac{\Lambda_H}{\mu_H} + H_{S,0}\, e^{-\mu_H t}$, which approaches $\frac{\Lambda_H}{\mu_H}$ as $t \to \infty$, $H_{S,0}$ is a constant and $A_S(t) = \frac{\Lambda_A}{\mu_A} + A_{S,0}\, e^{-\mu_A t}$, which approaches $\frac{\Lambda_A}{\mu_A}$ as $t \to \infty$, $A_{S,0}$ is a constant. Thus, all points converge at $X^* = \left(\frac{\Lambda_H}{\mu_H}, 0, \frac{\Lambda_A}{\mu_A}, 0\right)$. Hence, $X^* = \left(\frac{\Lambda_H}{\mu_H}, 0, \frac{\Lambda_A}{\mu_A}, 0\right)$ is globaly asymptotically stable. Moreover

$$D_Y G(X^*,0) = \begin{pmatrix} -(\alpha_H + \mu_H + \beta_H) & \frac{\delta_1 \Lambda_H}{\mu_H + m_1 \Lambda_H} \\ 0 & \frac{\delta_2 \Lambda_A}{\mu_A + m_3 \Lambda_A} - (\alpha_A + \mu_A + \beta_A) \end{pmatrix} \tag{20}$$

Therefore, from the formula in condition (ii), we get the following expression

$$\hat{G}(X,Y) = D_Y G(X^*,0)Y - G(X,Y) \tag{21}$$

and we obtain after some calculation

$$\hat{G}(X,Y)=\begin{pmatrix}\delta_1 A_I\left(\frac{\Lambda_H}{\mu_H+m_1\Lambda_H}-\frac{H_S(t)}{1+m_1H_S(t)+m_2A_I(t)}\right)\\ \delta_2 A_I\left(\frac{\Lambda_A}{\mu_A+m_3\Lambda_A}-\frac{A_S(t)}{1+m_3A_S(t)+m_4A_I(t)}\right)\end{pmatrix} \tag{22}$$

From the invariant region Ω, we have $\frac{\Lambda_H}{\mu_H}\geq H_S$ and $\frac{\Lambda_A}{\mu_A}\geq A_S$, therefore $\hat{G}(X,Y)\geq 0$ for all $(X,Y)\in\Omega$, and we conclude that the DFE is globally asymptotically stable whenever $\mathscr{R}_{ha}<1$.

3.6. Existence of Endemic equilibrium point. In this section, we explore the existence of the endemic equilibrium point (EE). In the presence of Cryptosporidiosis, $H_I(t)\neq 0$, $H_R(t)\neq 0$, $A_I(t)\neq 0$ and $A_R(t)\neq 0$, our model has an equilibrium point called endemic equilibrium point denoted by $E_1=(H_S^*,H_I^*,H_R^*,A_S^*,A_I^*,A_R^*)$. E_1 is the steady state solution where Cryptosporidiosis persist in the population of human and animal. For the existence of E_1, the elements must satisfy; $0<H_S^*$, $0<H_I^*$, $0<H_R^*$, $0<A_S^*$, $0<A_I^*$, $0<A_R^*$. We find the endemic equilibrium point by setting the right side of the model system equations (1) equal to zero, that is:

$$\Lambda_H-\mu_H H_S(t)-\frac{\delta_1 H_S(t)A_I(t)}{1+m_1H_S(t)+m_2A_I(t)}=0 \tag{23}$$

$$\frac{\delta_1 H_S(t)A_I(t)}{1+m_1H_S(t)+m_2A_I(t)}-(\alpha_H+\mu_H+\beta_H)H_I(t)=0 \tag{24}$$

$$\beta_H H_I(t)-\mu_H H_R(t)=0 \tag{25}$$

$$\Lambda_A-\mu_A A_S(t)-\frac{\delta_2 A_S(t)A_I(t)}{1+m_3A_S(t)+m_4A_I(t)}=0 \tag{26}$$

$$\frac{\delta_2 A_S(t)A_I(t)}{1+m_3A_S(t)+m_4A_I(t)}-(\alpha_A+\mu_A+\beta_A)A_I(t)=0 \tag{27}$$

$$\beta_A A_I(t)-\mu_A A_R(t)=0 \tag{28}$$

If $\mathscr{R}_{ha}>1$, the system (1) has a unique endemic equilibrium point given by:
$E_1=(H_S^*,H_I^*,H_R^*,A_S^*,A_I^*,A_R^*)$, where

$$A_S^*=\frac{\Lambda_A(\delta_2+m_4\mu_A\mathscr{R}_{ha}+m_4\Lambda_A\mathscr{R}_{ha})}{\mathscr{R}_{ha}(m_4\mu_A+\delta_2)(\mu_A+m_3\Lambda_A)-\delta_2 m_3\Lambda_A}>0 \tag{29}$$

since $\mathscr{R}_{ha} > 1$ this implies $\mathscr{R}_{ha}(m_4\mu_A + \delta_2)(\mu_A + m_3\Lambda_A) - \delta_2 m_3\Lambda_A > (m_4\mu_A + \delta_2)(\mu_A + m_3\Lambda_A) - \delta_2 m_3\Lambda_A = \mu_A(m_4\mu_A + \delta_2) + m_3 m_4\Lambda_A\mu_A > 0$,

$$A_I^* = \frac{\mathscr{R}_{ha}(\mu_A + m_3\Lambda_A)(\Lambda_A - \mu_A A_S^*)}{\delta_2\Lambda_A} > 0 \tag{30}$$

since $\frac{dA_S}{dt} < \Lambda_A - \mu_A A_S$,

$$A_R^* = \frac{\beta_A}{\mu_A}A_I^* > 0 \tag{31}$$

$$H_S^* = \frac{-(\mu_H(1+m_2A_I^*) + \delta_1 A_I^* - m_1\Lambda_H) + \sqrt{(\mu_H(1+m_2A_I^*) + \delta_1 A_I^* - m_1\Lambda_H)^2 + 4m_1\mu_H\Lambda_H(1+m_2A_I^*)}}{2m_1\mu_H} > 0 \tag{32}$$

$$H_I^* = \frac{\delta_2 H_S^* A_I^*}{(1+m_1H_S^* + m_2A_I^*)(\alpha_H + \mu_H + \beta_H)} > 0 \tag{33}$$

$$H_R^* = \frac{\beta_H}{\mu_H}H_I^* > 0 \tag{34}$$

3.7. Local stability of the Endemic equilibrium point. This section explores the local stability of the endemic equilibrium point E_1. We can see from (29),(30),(32), (33) that the endemic equilibrium point has long expressions and the standard linearization method which consist of finding the eigenvalues of the Jacobian matrix around the endemic equilibrium point can be mathematically complicated. Hence, in oder to investigate the local asymptotic stability of the endemic equilibrium point E_1, we use the result based on the center manifold theory described in [12, 13, 14] to investigate if the model system (1) exhibits a forward or backward bifurcation when $\mathscr{R}_{ha} = 1$. When bifurcution is forward, it implies that the endemic equilibrium point is locally asymptotically stable for $\mathscr{R}_{ha} > 1$. This result is reproduced here for convenience. To use that method we make the following simplification and change of variables in the system (1). Let $x_1 = H_S$, $x_2 = H_I$, $x_3 = H_R$, $x_4 = A_S$, $x_5 = A_I$ and $x_6 = A_R$. Futher by introducing the vector notation $x = (x_1,x_2,x_3,x_4,x_5,x_6)^T$, system (1) has the form $\frac{dx}{dt} = F(x)$, where $F=(f_1,f_2,f_3,f_4,f_5,f_6)^T$, as follows

$$\begin{cases} \frac{dx_1}{dt}=\Lambda_H-\mu_H x_1-\frac{\delta_1 x_1 x_5}{1+m_1x_1+m_2x_5}\\ \frac{dx_2}{dt}=\frac{\delta_1 x_1 x_5}{1+m_1x_1+m_2x_5}-(\alpha_H+\mu_H+\beta_H)x_2\\ \frac{dx_3}{dt}=\beta_H x_2-\mu_H x_3\\ \frac{dx_4}{dt}=\Lambda_A-\mu_A x_4-\frac{\delta_2 x_4 x_5}{1+m_3x_4+m_4x_5}\\ \frac{dx_5}{dt}=\frac{\delta_2 x_4 x_5}{1+m_3x_4+m_4x_5}-(\alpha_A+\mu_A+\beta_A)x_5\\ \frac{dx_6}{dt}=\beta_A x_5-\mu_A x_6 \end{cases} \tag{35}$$

We set the transmission rate δ_2 as the bifurcation parameter. Solving for δ_2 the equation $\mathscr{R}_{ha}=1$ gives $\delta_2=\delta_2^*$ as follows

$$\delta_2=\delta_2^*=\frac{(\mu_A+m_3\Lambda_A)(\alpha_A+\mu_A+\beta_A)}{\Lambda_A} \tag{36}$$

Linearisation of the system (35) at the disease-free equilibrium point $E_0=(\frac{\Lambda_H}{\mu_H},0,0,\frac{\Lambda_A}{\mu_A},0,0)$ with $\delta_2=\delta_2^*$ is

$$J(E_0)=\begin{pmatrix} -\mu_H & 0 & 0 & 0 & \frac{-\delta_1\Lambda_H}{\mu_H+m_1\Lambda_H} & 0\\ 0 & -(\alpha_H+\mu_H+\beta_H) & 0 & 0 & \frac{\delta_1\Lambda_H}{\mu_H+m_1\Lambda_H} & 0\\ 0 & \beta_H & -\mu_H & 0 & 0 & 0\\ 0 & 0 & 0 & -\mu_A & \frac{-\delta_2\Lambda_A}{\mu_A+m_3\Lambda_A} & 0\\ 0 & 0 & 0 & 0 & \frac{\delta_2\Lambda_A}{\mu_A+m_3\Lambda_A}-(\alpha_A+\mu_A+\beta_A) & 0\\ 0 & 0 & 0 & 0 & \beta_A & -\mu_A \end{pmatrix} \tag{37}$$

The above matrix $J(E_0)$ has a simple zero eigenvalues. Moreover, Let $v=(v_1,v_2,v_3,v_4,v_5,v_6)^T$ be the right eigenvector of (37) associated with the simple zero eigenvalue.Then v is obtained by solving $J(E_0)v=0$. By direct calculation, we get:

$$v=\left(\frac{-\delta_1\Lambda_H}{\mu_H(\mu_H+m_1\Lambda_H)}v_5,\frac{\delta_1\Lambda_H}{(\mu_H+m_1\Lambda_H)(\alpha_H+\mu_H+\beta_H)}v_5,\frac{-\delta_1\beta_H\Lambda_H}{\mu_H^2(\mu_H+m_1\Lambda_H)}v_5,\frac{-\delta_2\Lambda_A}{\mu_A(\mu_A+m_3\Lambda_A)}v_5,v_5,\frac{\beta_A}{\mu_A}v_5\right)^T \tag{38}$$

with $v_5=v_5>0$.

Let $z=(z_1,z_2,z_3,z_4,z_5,z_6)^T$ be the left eigenvector of (37) associated with the simple zero eigenvalue. It satisfies $zv=1$ and the matrix $J(E_0)$ should be transposed so that $J^T(E_0)z=0$.

By direct calculation, we get: $z = (0,0,0,0,0,z_5,0)^T$. Now $zv = 1$ gives $z_5 v_5 = 1$. Assume that $v_5 = \sigma > 0$, we obtain $z_5 = \frac{1}{\sigma}$. Then, the right and left eigenvectors turn out to be:

(39)
$$v = \left(\frac{-\delta_1 \Lambda_H \sigma}{\mu_H(\mu_H + m_1\Lambda_H)}, \frac{\delta_1 \Lambda_H \sigma}{(\mu_H + m_1\Lambda_H)(\alpha_H + \mu_H + \beta_H)}, \frac{-\delta_1 \beta_H \Lambda_H \sigma}{\mu_H^2(\mu_H + m_1\Lambda_H)}, \frac{-\delta_2 \Lambda_A \sigma}{\mu_A(\mu_A + m_3\Lambda_A)}, \sigma, \frac{\beta_A \sigma}{\mu_A}\right)^T$$

(40)
$$z = (0,0,0,0,0,\frac{1}{\sigma},0)^T$$

Now we have to compute a and b give by the formulae

(41)
$$a = \sum_{k,i,j=1}^{6} z_k v_i v_j \frac{\partial^2 f_k}{\partial x_i \partial x_j}(E_0, \delta_2^*) \ and \ b = \sum_{k,i=1}^{6} z_k v_i \frac{\partial^2 f_k}{\partial x_i \partial \delta_2^*}(E_0, \delta_2^*)$$

We will only consider $k = 5$ because $z_1 = z_2 = z_3 = z_4 = z_6 = 0$, that is the function $f_5 = \frac{\delta_2 x_4 x_5}{1+m_3x_4+m_4x_5} - (\alpha_A + \mu_A + \beta_A)x_5$. By direct calculation, we get:

(42)
$$a = -\frac{2\sigma(\alpha_A + \mu_A + \beta_A)^2}{\Lambda_A} < 0 \ and \ b = \frac{\Lambda_A}{\mu_A + m_3\Lambda_A} > 0$$

Therefore, $a < 0$ and $b > 0$ at bifurcation parameter $\delta_2 = \delta_2^*$. This scenario indicates that the Cryptosporidiosis model exhibits a forward bifurcation at $\mathscr{R}_{ha} = 1$. Its biological meaning is that as long as $\mathscr{R}_{ha} < 1$, the Cryptosporidiosis can be eliminated from the human and animal population. Hence the unique endemic equilibrium point $E_1 = (H_S^*, H_I^*, H_R^*, A_S^*, A_I^*, A_R^*)$ is locally asymptotically stable whenever $\mathscr{R}_{ha} > 1$.

3.7.1. *Bifurcation diagram.*

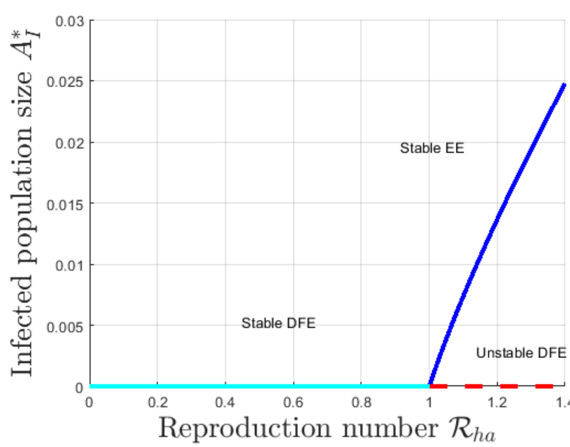

FIGURE 2. Forward bifurcation for Cryptosporidiosis model.

3.8. Global stability of the Endemic equilibrium point. In this section, we perform the global stability analysis of system (1) around the positive endemic equilibrium point using the method of Lyapunov functions with LaSalle'S invariant principle. Existing techniques for constructing Lyapunov functions have been improved by [15] because of the difficulties in constructing appropriate Lyapunov functions with nonlinear incidence.

Theorem 3.5 The Endemic equilibrium point E_1 of the model (1) is globally stable if $\mathscr{R}_{ha} > 1$, and condition (46) is hold.

Proof. We define the lyapunov function U as

$$\begin{aligned} U &= U(H_S,H_I,H_R,A_S,A_I,A_R) \\ &= \left(H_S - H_S^* - H_S^* ln\frac{H_S}{H_S^*}\right) + \left(H_I - H_I^* - H_I^* ln\frac{H_I}{H_I^*}\right) + \left(H_R - H_R^* - H_R^* ln\frac{H_R}{H_R^*}\right) \\ &\quad + \left(A_S - A_S^* - A_S^* ln\frac{A_S}{A_S^*}\right) + \left(A_I - A_I^* - A_I^* ln\frac{A_I}{A_I^*}\right) + \left(A_R - A_R^* - A_R^* ln\frac{A_R}{A_R^*}\right) \end{aligned} \tag{43}$$

Hence U is C^1 on the interior of Ω, E_1 is the global maximum of U on Ω, and we then have $U(H_S^*,H_I^*,H_R^*,A_S^*,A_I^*,A_R^*) = 0$. The time derivative of U alongside the solutions trajectories of system (1) is:

$$\begin{aligned} \frac{dU}{dt} &= \left(1 - \frac{H_S^*}{H_S}\right)\frac{dH_S}{dt} + \left(1 - \frac{H_I^*}{H_I}\right)\frac{dH_I}{dt} + \left(1 - \frac{H_R^*}{H_R}\right)\frac{dH_R}{dt} \\ &\quad + \left(1 - \frac{A_S^*}{A_S}\right)\frac{dA_S}{dt} + \left(1 - \frac{A_I^*}{A_I}\right)\frac{dA_I}{dt} + \left(1 - \frac{A_R^*}{A_R}\right)\frac{dA_R}{dt} \\ &= \left(1 - \frac{H_S^*}{H_S}\right)\left(\Lambda_H - \mu_H H_S - \frac{\delta_1 H_S A_I}{1 + m_1 H_S + m_2 A_I}\right) + \left(1 - \frac{H_R^*}{H_R}\right)(\beta_H H_I - \mu_H H_R) \\ &\quad + \left(1 - \frac{H_I^*}{H_I}\right)\left(\frac{\delta_1 H_S A_I}{1 + m_1 H_S + m_2 A_I} - (\alpha_H + \mu_H + \beta_H)H_I\right) \\ &\quad + \left(1 - \frac{A_S^*}{A_S}\right)\left(\Lambda_A - \mu_A A_S - \frac{\delta_2 A_S A_I}{1 + m_3 A_S + m_4 A_I}\right) + \left(1 - \frac{A_R^*}{A_R}\right)(\beta_A A_I - \mu_A A_R) \\ &\quad + \left(1 - \frac{A_I^*}{A_I}\right)\left(\frac{\delta_2 A_S A_I}{1 + m_3 A_S + m_4 A_I} - (\alpha_A + \mu_A + \beta_A)A_I\right) \end{aligned}$$

Separating positive and negative terms as U_1 and U_2, we have $\frac{dU}{dt} = U_1 - U_2$, where

$$\begin{aligned} U_1 &= \Lambda_H + \Lambda_A + \mu_H H_S^* + \mu_A A_S^* + \frac{\delta_1 A_I (H_S^* + H_S)}{1 + m_1 H_S + m_2 A_I} + \frac{\delta_2 A_I (A_S^* + A_S)}{1 + m_3 A_S + m_4 A_I} \\ &\quad + (\alpha_H + \mu_H + \beta_H)H_I^* + (\alpha_A + \mu_A + \beta_A)A_I^* + \beta_H H_I + \beta_A A_I + \mu_H H_R^* + \mu_A A_R^* \end{aligned} \tag{44}$$

and

$$
\begin{aligned}
U_2 = {} & \mu_H H_S + \mu_A A_S + \frac{\delta_1 H_S A_I}{1+m_1 H_S + m_2 A_I} + \frac{\delta_2 A_S A_I}{1+m_3 A_S + m_4 A_I} + \Lambda_H \frac{H_S^*}{H_S} + \Lambda_A \frac{A_S^*}{A_S} \\
& + (\alpha_H + \mu_H + \beta_H) H_I + (\alpha_A + \mu_A + \beta_A) A_I + \frac{\delta_1 H_S A_I H_I^*}{(1+m_1 H_S + m_2 A_I) H_I} + \mu_H H_R \\
& + \frac{\delta_2 A_S A_I A_I^*}{(1+m_3 A_S + m_4 A_I) A_I} + \mu_A A_R + \frac{\beta_H H_I H_R^*}{H_R} + \frac{\beta_A A_I A_R^*}{A_R}
\end{aligned}
\tag{45}
$$

If

$$
U_1 < U_2 \tag{46}
$$

then $\frac{dU}{dt} \leq 0$, $\frac{dU}{dt} = 0$ if and only if $H_S = H_S^*$, $H_I = H_I^*$, $H_R = H_R^*$, $A_S = A_S^*$, $A_I = A_I^*$, and $A_R = A_R^*$. The largest invariant set in

$$
\left\{ (H_S^*, H_I^*, H_R^*, A_S^*, A_I^*, A_R^*) \in \Omega; \frac{dU}{dt} = 0 \right\} \tag{47}
$$

is a singleton of E_1 with E_1 as the endemic equilibrium. Therefore by the LaSalle'S invariant principle, E_1 is globally asymptotically stable in Ω if $U_1 < U_2$.

3.9. Sensitivity analysis of the model parameters. In this section, we investigated the sensitivity of the parameters for the basic reproduction number of the model using the idea presented in [16, 17]. It is important to carry out the sensitivity of the basic reproduction number $\mathscr{R}_{ha}$ for its parameters. This will give parameters with a high impact on the Cryptosporidiosis model (1) and therefore allow to target on control measures to reduce the transmission of the disease. To measure the sensitivity index of $\mathscr{R}_{ha}$ to a given parameter p, we use the following relation:

$$
T_p^{\mathscr{R}_{ha}} = \left(\frac{\partial \mathscr{R}_{ha}}{\partial p} \right) \times \left(\frac{p}{\mathscr{R}_{ha}} \right) \tag{48}
$$

An analytical expression for the sensitivity index of each parameter involved in $\mathscr{R}_{ha}$ is derived as follows: $T_{\delta_2}^{\mathscr{R}_{ha}} = 1 > 0$, $T_{\Lambda_A}^{\mathscr{R}_{ha}} = 1 - \frac{m_3 \Lambda_A}{\mu_A m_3 \Lambda_A} > 0$, $T_{\alpha_A}^{\mathscr{R}_{ha}} = \frac{-\alpha_A}{\alpha_A + \mu_A + \beta_A} < 0$, $T_{\beta_A}^{\mathscr{R}_{ha}} = \frac{-\beta_A}{\alpha_A + \mu_A + \beta_A} < 0$, $T_{\mu_A}^{\mathscr{R}_{ha}} = -\mu_A \left(\frac{1}{\mu_A + m_3 \Lambda_A} + \frac{1}{\alpha_A + \mu_A + \beta_A} \right) < 0$.

In the following table of the parameters most are assumed (due to the lack of data) while few are taken from the literature.

Table 2. Parameter values for the model (1)

Parameter	Value	Source of data
Λ_H	2000/36500 per day	[18]
μ_H	5.48×10^{-5} per day	[20,21]
α_H	0.001 per day	[20,21]
β_H	0.1 per day	[20,21]
δ_1	2×10^{-6} per day	[18]
Λ_A	1000/245 per day	[18,19]
μ_A	1/245 per day	[18,19]
α_A	1/400 per day	[18]
β_A	0.1 per day	Assumed
δ_2	5.1×10^{-4} per day	[18]
m_1	0.01	Assumed
m_2	0.03	Assumed
m_3	0.01	Assumed
m_4	0.01	Assumed

Table 3. Sensitivity indices of $\mathscr{R}_{ha}$ with respect to the model parameters

Parameter	Value	Sens. index(+ve/-ve)
δ_2	5.1×10^{-4}	1
Λ_A	1000/245	0.0909
m_3	0.01	-0.90909
α_A	1/400	-0.02345
μ_A	1/245	-0.129204
β_A	0.1	-0.93824

From Table 3, we can observe that only the parameter δ_2, has the most positive influence on $\mathscr{R}_{ha}$. This means that the increase of this parameter while keeping other parameters constant will increase the value of $\mathscr{R}_{ha}$ leading to an increase of the spread of Cryptosporidiosis in the human and animal population. We likewise observe that the parameters m_3, α_A, μ_A and β_A respectively have the most negative impact on $\mathscr{R}_{ha}$. This implies that the increase of these parameters while keeping the other constant will decrease the value of $\mathscr{R}_{ha}$, meaning that they will decrease the endemicity of Cryptosporidiosis in the human and animal population.

4. NUMERICAL SIMULATIONS

We performed numerical simulations of our proposed model (1) to support some of the analytical results. We use the set of parameters values given in Table 2 and the initial values of the model are set as: $H_S(0) = 1000, H_I(0) = 10, H_R(0) = 5, A_S(0) = 50, A_I(0) = 500, A_R(0) = 10$. We set the final time as $t_f = 120$ days. This was chosen on the basis of the assumption that a period of four month is enough for the disease spread. All simulations are done using Matlab with the ode45 function.

4.1. Simulation of the population dynamics of the Cryptosporidiosis showing the existence of a unique endemic equilibrium point (EE) when $\mathscr{R}_{ha} > 1$. We observe from Figure 3 that whenever $\mathscr{R}_{ha} > 1$, the susceptible humans population drop exponentially and converges to a steady state to acquire endemic equilibrium level while the infected humans increase exponentially to a certain maximum point before exponential drop to a certain endemic level. This is an indicator of Cryptosporidiosis outbreak. We also observe that the susceptible animals population decrease exponentially due to natural death and acquisition of Cryptosporidiosis infection and finally acquire the endemic equilibrium level. Hence, without intervention the populations approach the endemic equilibrium levels in the long run implying the existence and stability of endemic equilibrium point.

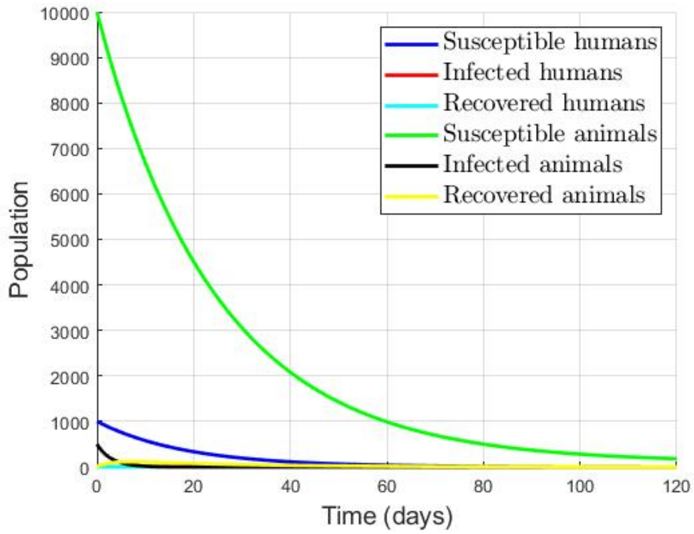

FIGURE 3. Graph showing the population dynamics.

4.2. Simulation of the effects of transmission rate (δ_1) on susceptible and infected humans. Figure 4 shows the simulation of the model by varying the value of the transmission rate from infected animals to susceptible humans (δ_1) to see its effects on the susceptible and infected humans. From Figure 4 (A), we observe that as the value of (δ_1) increases, the number of susceptible humans decreases and from Figure 4 (B), we see that the number of infected humans increases as the value of (δ_1) increases, leading to the increase of the basic reproduction number $\mathscr{R}_{ha}$ which also ascertain the sensitivity analysis.

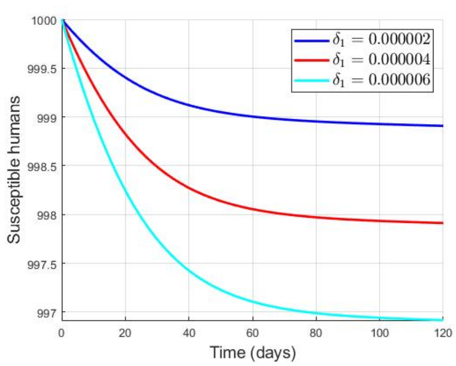

(A)

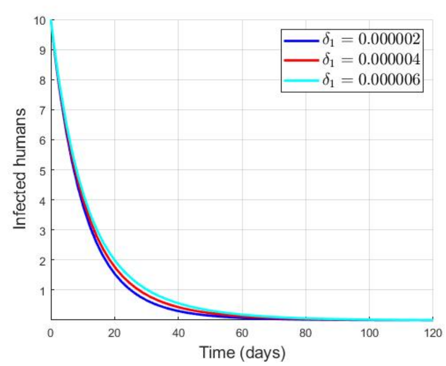

(B)

FIGURE 4. Graph of the effects of transmission rate (δ_1) on susceptible and infected humans.

4.3. Simulation of the effects of transmission rate (δ_2) on infected animals and infected humans. Figure 5 depicts the simulation results of the model by varying the value of transmission rate from infected animals to healthy animals (δ_2) to see its effects on the infected animals and infected humans. We observe from Figure 5 (A) and Figure 5 (B) that the number of infected humans along with the number of infected animals increase as the transmission rate (δ_2) increases, leading to the increase of the basic reproduction number $\mathscr{R}_{ha}$.

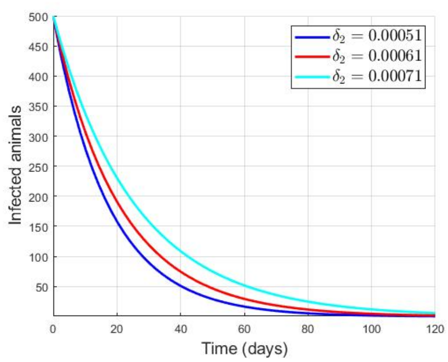

(A)

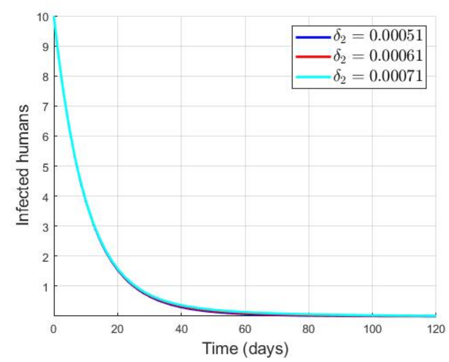

(B)

FIGURE 5. Graph of the effects of transmission rate (δ_2) on infected animals and infected humans.

4.4. Simulation of the effects of saturation level m_1 and m_2 on the infected humans population. From the analytical results, we observed that the saturation levels m_1 and m_2 do not contribute on the basic reproduction number $\mathscr{R}_{ha}$, but they have the effects on infected population. Figure 6 is simulation results of the model showing the effects of the saturation levels m_1 and m_2 on the infected humans population. We observe that an increase in m_1 (Figure 6 (A)) and m_2 (Figure 6 (B)), respectively produces a decrease in the number of infected humans. In this fact, the saturation levels ultimately affect the dynamics of the model system and then, minimizing contacts between infected and susceptible populations are highly recommended.

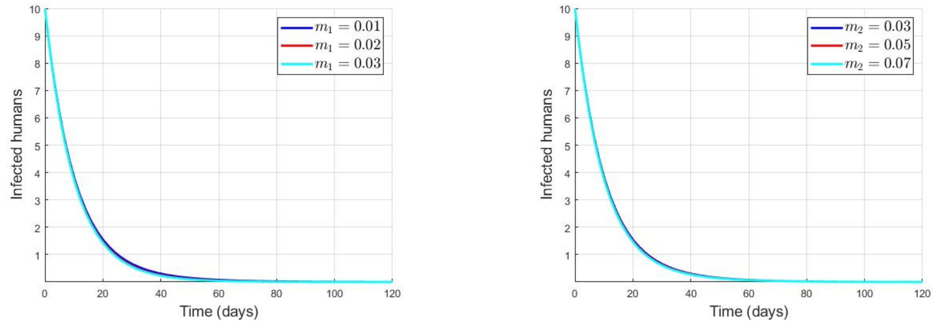

(A) (B)

FIGURE 6. Graph showing the effect of saturation levels m_1 and m_2 on the infected humans population.

4.5. Simulation of the effects of saturation level m_3 and m_4 on the infected animals population. From the analytical results, we observed that the saturation levels m_3 contribute on the basic reproduction number and m_4 do not contribute on the basic reproduction number $\mathscr{R}_{ha}$, but they have the effects on infected population. Figure 7 is simulation results of the model showing the effects of the saturation levels m_3 and m_4 on the infected animals population. We observe that an increase in m_3 (Figure 7 (A)) and m_4 (Figure 7 (B)), respectively produces a decrease in the number of infected animals. In this fact, the saturation levels ultimately affect the dynamics of the model system and then, minimizing contacts between infected and susceptible populations are highly recommended.

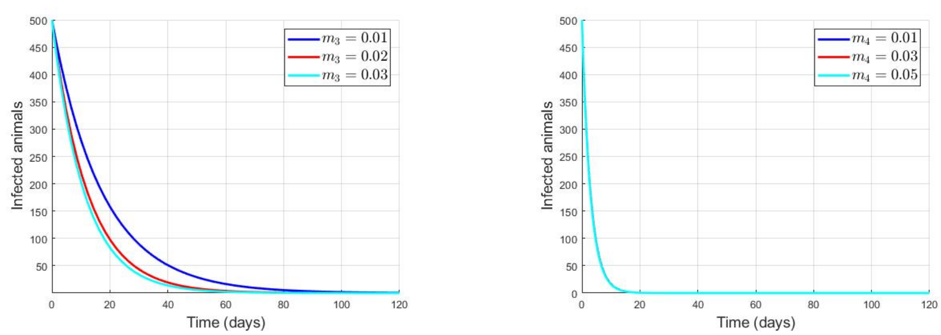

(A) (B)

FIGURE 7. Graph showing the effect of saturation levels m_3 and m_4 on the infected animals population.

4.6. Simulation of the effects of natural death of animals μ_A, and disease induced mortality α_A on the infected animals population. Figure 8 is drawn by varying the value of (μ_A) and (α_A) to show its effects on the infected animals population. It is observed from both Figure 8 (A) and Figure 8 (B) that the increase in the values of μ_A and α_A, respectively decrease the number of infected animals leading to the decrease of the basic reproduction number $\mathscr{R}_{ha}$ which also ascertain the sensitivity analysis result.

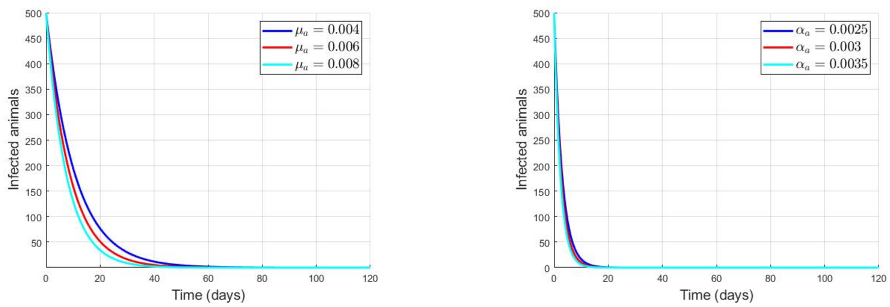

(A) (B)

FIGURE 8. Graph showing the effects of μ_A and α_A on infected animals.

4.7. Simulation of the effects of harvesting μ_H, and disease induced mortality on the infected humans. Figure 9 is the simulation results of the model showing the effects of harvesting of humans μ_H and the disease induced mortality rate α_H on the infected humans population. From Figure 9 (A) and Figure 9 (B), we observe that an increase in α_H and μ_H, respectively produces a decrease in the number of infected humans. This leads to the decrease of the basic reproduction number $\mathscr{R}_{ha}$ which also validate the sensitivity analysis result.

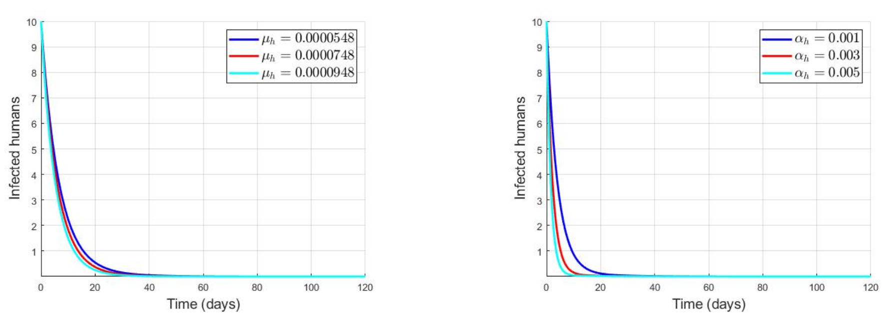

(A) (B)

FIGURE 9. Graph showing the effects of μ_H and α_H on infected humans.

5. Discussions and Conclusions

In this paper, we have formulated and analyzed a mathematical model describing the transmission dynamics of Cryptosporidiosis disease in human and animal population with Beddington-DeAngelis incidence function. We computed the basic reproduction number $(\mathscr{R}_{ha})$ which led to the following findings: the disease-free equilibrium (E_0) is locally asymptotically stable if $\mathscr{R}_{ha} < 1$, as confirmed by the Routh-Hurwitz criterion, and the endemic equilibrium (E_1) is globally asymptotically stable if $\mathscr{R}_{ha} > 1$, as confirmed by Lyapunov's method and LaSalle's invariance principle. Further, we applied the center manifold theory to establish that the model undergoes the forward bifurcation at $\mathscr{R}_{ha} = 1$. Computationally, we performed sensitivity analysis of the threshold quantity $(\mathscr{R}_{ha})$ and the results showed that only the parameter (δ_2) has the most sensitive to the spread of Cryptosporidiosis. The rate of Cryptosporidiosis infection can be reduced by ensuring that the rate of interaction between susceptible humans and infected animals, (δ_1) is minimised. Moreover, the spread of Cryptosporidiosis infection can be curbed by reducing the rate of interaction between susceptible animals and contact with infected animals. The proposed model is not exhaustive. Following some authors who considered that in the persistent mode of transmission, the infection process of human or animal by protozoan parasites Cryptosporidium takes time for the appearance of disease symptoms, we plan to use this assumption to study the existence of periodic solutions of the model. Hence, in our next paper, we will increase realism by exploring the effects of time delays on the dynamics of Cryptosporidiosis.

Conflict of Interests

The authors declare that there is no conflict of interests.

References

[1] S.J. Pereira, N.E. Ramirez, L. Xiao, et al. Pathogenesis of human and bovinecryptosporidium parvumin gnotobiotic pigs, J. Infect. Dis. 186 (2002), 715–718. https://doi.org/10.1086/342296.

[2] E.T. Pamo, Country pasture/forage resource profiles Cameroon, in: J.M. Suttle, S.G. Reynolds (eds.), FAO, Rome, 2008.

[3] R. Fayer, L. Xiao, Cryptosporidium and cryptosporidiosis, CRC Press, Boca Raton, 2008.

[4] S. Tzipori, H. Ward, Cryptosporidiosis: biology, pathogenesis and disease, Microbes Infect. 4 (2002), 1047–1058. https://doi.org/10.1016/s1286-4579(02)01629-5.

[5] S. Tzipori, J. Griffiths, Natural history and biology of cryptosporidium parvum, Adv. Parasitol. 40 (1998), 5–36. https://doi.org/10.1016/s0065-308x(08)60116-5.

[6] M.A. Brookhart, A.E. Hubbard, M.J. van der Laan, et al. Statistical estimation of parameters in a disease transmission model: analysis of aCryptosporidium outbreak, Stat. Med. 21 (2002), 3627–3638. https://doi.org/10.1002/sim.1258.

[7] S. Tzipori, J. Griffiths, Natural history and biology of cryptosporidium parvum, Adv. Parasitol. 40 (1998), 5–36. https://doi.org/10.1016/s0065-308x(08)60116-5.

[8] S. Tzipori, H. Ward, Cryptosporidiosis: biology, pathogenesis and disease, Microbes Infect. 4 (2002), 1047–1058. https://doi.org/10.1016/s1286-4579(02)01629-5.

[9] D.W. Muia, S. Osman, M. Wainaina, Modelling and analysis of trypanosomiasis transmission mechanism, Glob. J. Pure Appl. Math. 14 (2018), 1311–1331.

[10] O.D. Makinde, K.O. Okosun, Impact of chemo-therapy on optimal control of malaria disease with infected immigrants, Biosystems. 104 (2011), 32–41. https://doi.org/10.1016/j.biosystems.2010.12.010.

[11] B.N. Nyasagare, S. Osman, M. Wainaina, Modelling and analysis of campylobacteriosis in human and animal populations, Glob. J. Pure Appl. Math. 15 (2019), 551–567.

[12] C. Castillo-Chavez, B. Song, Dynamical models of tuberculosis and their applications, Math. Biosci. Eng. 1 (2004), 361–404.

[13] T. Kinene, L.S. Luboobi, B. Nannyonga, et al. A mathematical model for the dynamics and cost effectiveness of the current controls of cassava brown streak disease in Uganda, J. Math. Comput. Sci. 5 (2015), 567–600.

[14] P.C. Kawe, O.J. Abonyo, D.M. Malonza, et al. Modeling and stability analysis of an eco-epidemiological model of IYSV disease dynamics in onion plants with nonlinear saturated incidence rate and logistic growth, Glob. J. Pure Appl. Math. 18 (2022), 171-204.

[15] C. Vargas-De-León, On the global stability of SIS, SIR and SIRS epidemic models with standard incidence, Chaos Solitons Fractals. 44 (2011), 1106–1110. https://doi.org/10.1016/j.chaos.2011.09.002.

[16] D. Aldila, M. Angelina, Optimal control problem and backward bifurcation on malaria transmission with vector bias, Heliyon. 7 (2021), e06824. https://doi.org/10.1016/j.heliyon.2021.e06824.

[17] S. Osman, D. Otoo, O.D. Makinde, Modeling anthrax with optimal control and cost effectiveness analysis, Appl. Math. 11 (2020), 255–275. https://doi.org/10.4236/am.2020.113020.

[18] F. Chen, J. Cui, Cross-species epidemic dynamic model of influenza, in: 2016 9th International Congress on Image and Signal Processing, BioMedical Engineering and Informatics (CISP-BMEI), IEEE, Datong, China, 2016: pp. 1567–1572. https://doi.org/10.1109/CISP-BMEI.2016.7852965.

[19] China Agricultural Yearbook Editing Committee, China agriculture yearbook, China Agriculture Press, Beijing, (2012).

[20] S. Liu, S. Ruan, X. Zhang, Nonlinear dynamics of avian influenza epidemic models, Math. Biosci. 283 (2017), 118–135. https://doi.org/10.1016/j.mbs.2016.11.014.

[21] X. Zhang, Global dynamics of a stochastic avian–human influenza epidemic model with logistic growth for avian population, Nonlinear Dyn. 90 (2017), 2331–2343. https://doi.org/10.1007/s11071-017-3806-5.